Marcelo A. Trindade

trindade@sc.usp.br
Department of Mechanical Engineering
São Carlos School of Engineering
University of São Paulo
13566-590 São Carlos, SP, Brazil

Ayech Benjeddou

benjeddou@supmeca.fr
Institut Supérieur de Mécanique de Paris
LISMMA/Structures
3 rue Fernand Hainault
93407 Saint Ouen, France

Parametric Analysis of Effective Material Properties of Thickness-Shear Piezoelectric Macro-Fibre Composites

A previous study on the characterization of effective material properties of a d_{15} thickness-shear piezoelectric Macro-Fibre Composite (MFC) made of seven layers (Kapton, Acrylic, Electrode, Piezoceramic Fibre and Epoxy Composite, Electrode, Acrylic, Kapton) using a finite element homogenization method has shown that the packaging reduces significantly the shear stiffness of the piezoceramic material and, thus, leads to significantly smaller effective electromechanical coupling coefficient k_{15} and piezoelectric stress constant e_{15} when compared to the piezoceramic fibre properties. Therefore, the main objective of this work is to perform a parametric analysis in which the effect of the variations of fibre volume fraction, Epoxy elastic modulus, electrode thickness and active layer thickness on the MFC effective material properties is evaluated. Results indicate that an effective d_{15} MFC should use relatively thick fibres having relatively high shear modulus and relatively stiff epoxy filler. On the other hand, the electrode thickness does not affect significantly the MFC performance.
Keywords: macro-fibre composites, shear actuators, properties characterization, finite element homogenization method

Introduction

Over the last decade, packaged conformable piezoelectric sensors and actuators have drawn great attention from the research community working on applications such as structural control, structural health monitoring and energy harvesting. For practical and commercial applications, they do possess a number of advantages over the standard monolithic piezoceramic patches, such as a less brittle behaviour and more robust electric connection (Skinner, Newnham and Cross, 1978). Based on the concept of Piezoelectric Fibre Composites (PFC) proposed by Bent and Hagood (1997), who used extruded piezoceramic fibres with circular cross-section embedded to an epoxy-based resin matrix and covered by Copper electrodes and protective Kapton and/or Acrylic layers, the so-called Macro-Fibre Composites (MFC) have become very popular since they combine the conformability of epoxy-matrix composites and the electromechanical energy density of piezoceramic materials (Wilkie, Bryant and High, 2000). The MFCs replace the extruded piezoceramic fibres of PFC by machined (diced) rectangular fibres of a piezoceramic material. This innovation led to a cheaper and more reliable manufacturing process and allowed direct contact between fibres and electrodes, solving the main problem of permittivity mismatch of PFCs. The original MFC idea developed at NASA (Wilkie, Bryant and High, 2000) uses Interdigitated Electrodes (IDE) to induce longitudinal or 33 mode in the fibres. But, nowadays, it is possible to find MFCs using uniform field (continuous) electrodes that operate with the transverse or 31 mode in the fibres.

Beside the two above longitudinal and transverse piezoelectric responses, the third one is the so-called transverse shear mode, or thickness shear mode, which can be obtained by the application of an electric field that is perpendicular to the remanent polarization direction. This leads to a rotation of the electrical dipoles which induces shear stresses/strains in the material. The transverse shear mode in commercially available piezoceramic patches is normally obtained by polarization along the length or width direction followed by removal of the electrodes used for polarization and deposition of new electrodes on the top and bottom surfaces. The presence of the new electrodes imposes a dominant electric field, either applied

or induced, in the thickness direction, thus perpendicular to the length or width poling direction. Since the mid-90s, the shear mode of monolithic piezoceramic materials has been considered for applications in the design of smart structures (Sun and Zhang, 1995; Benjeddou, Trindade and Ohayon, 1997; Benjeddou, 2007; Trindade and Benjeddou, 2009), including active (Benjeddou, Trindade and Ohayon, 2000; Raja, Prathap and Sinha, 2002; Baillargeon and Vel, 2005), passive (Benjeddou and Ranger, 2006; Trindade and Maio, 2008) and active-passive (Trindade, 2011; Santos and Trindade, 2011) vibration control. From these studies, the shear mode seems to be an interesting alternative for stiffer structures, higher frequencies and non-standard shape deflection patterns.

To take advantage of the high piezoelectric coupling constant d_{15} that most piezoceramic materials have and the fact that it couples directly to transverse shear strains, an alternative MFC design, in which the macro-fibres are oriented perpendicular to the direction of motion, was recently proposed by Raja and Ikeda (2008) to induce the transverse shear mode (15 or 35) in the piezoceramic fibres. It was named as Shear Actuated Fibre Composite (SAFC). The same authors later applied theoretically the proposed design for the vibration control of laminate structures (Raja, Ikeda and Dwarakanathan, 2011). The SAFC basically consists of piezoceramic fibres with poling direction perpendicular to the fibre longitudinal axis, as for the d_{33} MFC, but instead of orienting the fibres along the longitudinal direction of the actuator, the fibres are oriented along the width of the actuator so that poling direction is in the longitudinal direction of the actuator, as shown in Fig. 1. Different from the IDE proposition of Raja and Ikeda (2008), a continuous (Fig. 1a) or woven-type (Fig. 1b) electrode, such as those used in commercial d_{31} MFCs, can be used to induce a uniform electric field in the direction of the actuator thickness (Benjeddou and Al-Ajmi, 2009; Trindade and Benjeddou, 2011). As the fibres are poled in their width direction, that is, the longitudinal direction of the actuator, a shear strain is induced in the fibres transversal planes. The width-poled piezoceramic fibres can be made by dice cutting either thickness-poled or longitudinal- or width-poled piezoceramic plates. However, in the first case, proposed by Raja and Ikeda (2008), the resulting fibres should be rotated 90° around their axes before positioning them in the Epoxy-Copper electrode layer, so that the poling direction of each fibre coincides with the longitudinal direction of the actuator, which can

be difficult in practice. In the second case, several width-poled plates can be aligned in the polymer film frame before dice cutting of the ensemble leading to a probably cheaper process to produce aligned fibres poled in the width direction, which after packaging would be the longitudinal direction of the actuator.
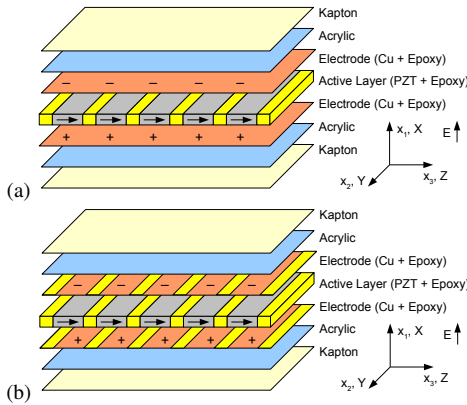

Figure 1. Schematic representations of thickness-shear "d_{15}" Macro-Fibre Composite with (a) continuous or homogeneous electrodes (Trindade and Benjeddou, 2011) and (b) discontinuous or heterogeneous electrodes (presently proposed).

One of the main difficulties in the study of MFCs, as an alternative to monolithic piezoceramic patches, is that their behaviour may be much more complex since they are made of several different materials (piezoceramic fibres, epoxy matrix, electrode layers and protective layers). Therefore, it is necessary to understand and model their behaviour to be able to quantify or characterize their effective material properties and, thus, their effectiveness as distributed sensors and actuators. Recently, some research effort has been directed towards the identification and characterization of such transducers, in extension (33 or 31) (Deraemaeker et al., 2007, 2009; Deraemaeker and Nasser, 2010; Biscani et al., 2011) and transverse shear (15) (Benjeddou and Al-Ajmi, 2009) modes. It has been shown that the effective properties depend not only on the piezoceramic material used for the fibres and epoxy material used for the matrix and epoxy-to-piezoceramic volume fraction, but also on the geometrical and material properties of the other layers (Kapton, Acrylic, Electrodes). Some analytical methods from the composite materials literature, such as the Asymptotic Homogenization Method (AHM) (Benjeddou and Al-Ajmi, 2009; Otero et al., 2005) and the Uniform Field Method (UFM) (Bent and Hagood, 1997) can be applied to obtain the effective properties of the composite transducer active core from the properties of its components. Alternatively, one may use techniques based on finite element modelling of the composite transducer active core to identify its effective properties (Berger et al., 2005).

A previous study of a shear actuated d_{15} MFC made of seven layers (Kapton, Acrylic, Electrode, Piezoceramic Fibre and Epoxy Composite, Electrode, Acrylic, Kapton) using a finite element homogenization method to characterize its effective material properties was presented in Trindade and Benjeddou (2011). It has been shown that the packaging reduces significantly the shear stiffness of the piezoceramic material and, thus, leads to significantly smaller effective electromechanical coupling coefficient k_{15} and piezoelectric stress constant e_{15} when compared to the piezoceramic fibre properties. However, it was found that the piezoelectric charge constant d_{15} is less affected by the softer layers required by the MFC packaging. This work presents, first, an analysis similar to the previous one (Trindade and Benjeddou, 2011) but using another

electrode design and, second, a parametric analysis in which the effect of the variations of fibre volume fraction, Epoxy elastic modulus, electrode thickness and active layer thickness on the effective material properties is evaluated.

Shear Electromechanical Coupling

The shear or d_{15} response mode requires the poling vector P and main electric field E to be perpendicular to each other. From the modelling point of view, this can be achieved as in Fig. 1, by positioning reference axes such that the poling direction, width of fibre or length of actuator, coincides with direction x_3 or z and the fibre thickness, and actuator thickness, coincides with direction x_1 or x. These reference system and electric configuration provide easy results interpretation as compared to commercial MFCs and standard piezoelectricity notation.

For a linear orthotropic piezoelectric material poled in x_3 direction and electrodes fully covering top (x_1^+) and bottom (x_1^-) surfaces such that a preferential or dominant x_1 direction is imposed for the electric field and displacement, so that $E_2 = E_3 = 0$, the constitutive equations can be written in the mixed e-form type, as

$$
\begin{Bmatrix} T_1 \\ T_2 \\ T_3 \\ T_4 \\ T_5 \\ T_6 \\ \hline D_1 \end{Bmatrix} =
$$

$$
\begin{bmatrix}
c_{11}^E & c_{12}^E & c_{13}^E & 0 & 0 & 0 & 0 \\
c_{12}^E & c_{22}^E & c_{23}^E & 0 & 0 & 0 & 0 \\
c_{13}^E & c_{23}^E & c_{33}^E & 0 & 0 & 0 & 0 \\
0 & 0 & 0 & c_{44}^E & 0 & 0 & 0 \\
0 & 0 & 0 & 0 & c_{55}^E & 0 & -e_{15} \\
0 & 0 & 0 & 0 & 0 & c_{66}^E & 0 \\
\hline
0 & 0 & 0 & 0 & e_{15} & 0 & \epsilon_{11}^S
\end{bmatrix}
\begin{Bmatrix} S_1 \\ S_2 \\ S_3 \\ S_4 \\ S_5 \\ S_6 \\ \hline E_1 \end{Bmatrix}. \quad (1)
$$

where T_p and S_q, with $p, q = 1, \ldots, 6$, denote the six components of mechanical stress and strain vectors in Voigt notation. D_1 and E_1 denote the electric displacement and field. c_{pq}^E, e_{15} and ϵ_{11}^S denote the elastic stiffness (at constant electric fields), piezoelectric and electric permittivity (at constant mechanical strains) constants.

The electromechanical coupling is then between the electric field and displacement in x_1 direction, E_1 and D_1, and $x_1 - x_3$ shear stress and strain, T_5 and S_5. Thus, this is known as '15' operation mode. The electromechanical coupling coefficient can be defined from the value of the coupling or interaction coefficient relative to the principal or diagonal coefficients (Ikeda, 1990) using the standard intensive d-form type of the constitutive equations, such that

$$
k_{15}^2 = \frac{d_{15}^2}{s_{55}^E \epsilon_{11}^T}, \quad (2)
$$

where

$$
d_{15} = e_{15}/c_{55}^E, \quad s_{55}^E = 1/c_{55}^E \text{ and } \epsilon_{11}^T = \epsilon_{11}^S + e_{15}^2/c_{55}^E. \quad (3)
$$

It is thus clear that the material properties d_{15}, c_{55}^E and ϵ_{11}^T are of major importance for the evaluation of the potential of such material as a candidate for the development of actuators and sensors. Table 1 presents typical values of these constants for a number of commercially available piezoceramic materials.

Table 1. Shear mode d_{15} properties of some commercially available piezoceramic materials (Trindade and Benjeddou, 2011).

	c_{55}^E (GPa)	$\epsilon_{11}^T/\epsilon_0$	d_{15} (pC/N)	e_{15} (C/m^2)	k_{15}^2 (%)	k_{15}
APC-840	26.9	1427	480	13.6	49.0	0.70
APC-850	21.8	1851	590	13.2	46.2	0.68
APC-855	22.4	3012	720	15.0	43.6	0.66
EC-76	21.9	2853	730	16.0	46.2	0.68
EC-64	25.7	1436	506	13.0	51.8	0.72
PIC-255	21.0	1650	550	11.6	43.6	0.66
PZT-5H	23.0	3130	740	17.0	45.6	0.68
PZT-5A	21.1	1730	584	12.3	46.9	0.68
PZT-7A	29.4	930	360	10.6	46.2	0.68
Sonox-P502	30.1	1950	560	16.9	54.8	0.74
Sonox-P504	24.8	1920	530	13.2	43.6	0.66
Sonox-P508	29.8	1700	550	16.4	50.4	0.71

In the case of d_{15} MFCs which are composed of a number of materials, it is important to identify the effective properties of the ensemble based on its constituents properties. For that, the Representative Volume Element (RVE) technique together with Ansys$^{(R)}$ finite element software is used to evaluate effective material properties of multilayer d_{15} MFCs.

Finite Element Homogenization Technique

In this section, the recently proposed (Trindade and Benjeddou, 2011) finite element homogenization technique is applied to evaluate the effective properties of a d_{15} MFC including the electrode and protective layers, according to the schematic representation of Fig. 1(b) that shows the new electrode configuration adopted here. It consists in imposing relative mechanical displacement conditions, including symmetry (or periodicity), on the boundaries of the RVE $(X_1^-, X_1^+, X_2^-, X_2^+, X_3^-, X_3^+)$. In addition, electric potential boundary conditions are imposed at the electrodes on surfaces X_1^{e-} and X_1^{e+}. Relative potentials are also imposed on the other boundaries as symmetry (or periodicity) conditions. In case of the RVE considered for the d_{15} MFC, shown in Fig. 2, these boundaries are X_1^-: $x_1 = 0$, X_1^+: $x_1 = h_P + 2(h_E + h_A + h_K)$, X_2^-: $x_2 = 0$, X_2^+: $x_2 = w$, X_3^-: $x_3 = 0$, X_3^+: $x_3 = L_P + L_E$, X_1^{e-}: $x_1 = h_E + h_A + h_K$, X_1^{e+}: $x_1 = h_P + h_E + h_A + h_K$.

The protective layers, made of Kapton and Acrylic materials, and electrode layer, made of Copper and Epoxy, are considered isotropic. Notice that the isotropy of the electrode layer depends on its design. Electrode designs such as those used for d_{31} MFC (continuous or woven-type) seem to be more reasonable than those used for the d_{33} MFC (interdigitated), since the voltage should ideally be constant all over the fibre surfaces. An isotropic continuous electrode (Fig. 1(a)) was considered in a previous work (Trindade and Benjeddou, 2011), but, in this work, a discontinuous electrode (Epoxy/Copper/Epoxy) is considered (Fig. 1(b)).

Average strains and electric fields can therefore be imposed to the RVE using displacements and voltage boundary conditions, such that

$$u_i^{X_j^+} - u_i^{X_j^-} = \bar{S}_{ij}(x_j^{X_j^+} - x_j^{X_j^-}), \ i,j = 1,2,3, \quad (4)$$

and

$$\phi^{X_1^+} - \phi^{X_1^-} = -\bar{E}_1(x_1^{X_1^+} - x_1^{X_1^-}). \quad (5)$$

The resulting average strains, stresses, electric fields and electric displacements in the RVE are defined as

$$\bar{S}_q = \frac{1}{V}\int_V S_q \, dV, \ \bar{T}_p = \frac{1}{V}\int_V T_p \, dV, \text{ with } p,q = 1,\dots,6, \quad (6)$$

$$\bar{E}_k = \frac{1}{V}\int_V E_k \, dV, \ \bar{D}_i = \frac{1}{V}\int_V D_i \, dV, \text{ with } i,k = 1,2,3. \quad (7)$$

These integrals are approximated in Ansys$^{(R)}$ by a sum over averaged element values multiplied by the respective element volume divided by total volume of the RVE, such that

$$\bar{S}_q = \frac{\sum_{e=1}^N S_q^{(e)} V^{(e)}}{\sum_{e=1}^N V^{(e)}}, \ \bar{T}_p = \frac{\sum_{e=1}^N T_p^{(e)} V^{(e)}}{\sum_{e=1}^N V^{(e)}}, \text{ with } p,q = 1,\dots,6, \quad (8)$$

$$\bar{E}_k = \frac{\sum_{e=1}^N E_k^{(e)} V^{(e)}}{\sum_{e=1}^N V^{(e)}}, \ \bar{D}_i = \frac{\sum_{e=1}^N D_i^{(e)} V^{(e)}}{\sum_{e=1}^N V^{(e)}}, \text{ with } i,k = 1,2,3. \quad (9)$$

where $V^{(e)}$ is the volume of the element e. $S_q^{(e)}$, $T_p^{(e)}$, $E_k^{(e)}$ and $D_i^{(e)}$ are the average strains, stresses, electric fields and electric displacements evaluated at element e. N is the total number of finite elements used to discretize the RVE.

For the evaluation of the elastic constants related to normal strains and stresses c_{pq}^E, $p,q = 1,2,3$, three local problems are analysed, for which a normal strain S_q $(q = 1,2,3)$ is applied by imposing relative normal displacements $u_q^{X_q^+} - u_q^{X_q^-}$. In order to obtain $\bar{S}_j = 0$ if $j \neq q$, the normal displacements u_j for each pair of nodes at opposing surfaces X_j^- and X_j^+ are set to be equal (symmetrically coupled degrees of freedom). Then, considering the constitutive equations in (1), the effective elastic constants are evaluated using the following expressions

$$c_{pq}^E = \bar{T}_p/\bar{S}_q, \ p,q, = 1,2,3, \quad (10)$$

where the average stresses $\bar{T}_p$ and strains $\bar{S}_q$ are evaluated using (8).

For the evaluation of the elastic constants related to shear strains and stresses c_{pp}^E, $p = 4,5,6$, other three local problems are analysed for which shear strains S_{ik} $(S_{23} = S_4/2, S_{13} = S_5/2$ and $S_{12} = S_6/2)$ are applied to approximate a pure shear stress state in the planes $x_2 - x_3$, $x_1 - x_3$ and $x_1 - x_2$ by imposing relative shear displacements $u_i^{X_k^+} - u_i^{X_k^-}$ at surfaces X_k^+/X_k^- and $u_k^{X_i^+} - u_k^{X_i^-}$ at surfaces X_i^+/X_i^-. Moreover, the normal displacements at the boundary surfaces parallel to each shear plane of interest are symmetrically coupled to ensure zero strains perpendicular to the shear plane. Therefore, the effective elastic constants are evaluated in terms of the average shear stresses $\bar{T}_p$ and strains $\bar{S}_p$ using

$$c_{pp}^E = \bar{T}_p/\bar{S}_p, \ p = 4,5,6. \quad (11)$$

Table 2. Boundary conditions (displacement/electric potential) and relations used to evaluate the effective material properties of a d_{15} piezoelectric MFC.

Problem	X_1^-/X_1^+	X_2^-/X_2^+	X_3^-/X_3^+	X_1^{e-}/X_1^{e+}	Relation
1	$u_1^{i+} - u_1^{i-} = q$	$u_2^{i+} - u_2^{i-} = 0$	$u_3^{i+} - u_3^{i-} = 0$	-	$c_{1j}^E = \bar{T}_j/\bar{S}_1$ (10)
	-	$\phi^{i+} - \phi^{i-} = 0$	$\phi^{i+} - \phi^{i-} = 0$	$\phi^{i+} = 0; \phi^{i-} = 0$	
2	$u_1^{i+} - u_1^{i-} = 0$	$u_2^{i+} - u_2^{i-} = q$	$u_3^{i+} - u_3^{i-} = 0$	-	$c_{2j}^E = \bar{T}_j/\bar{S}_2$ (10)
	-	$\phi^{i+} - \phi^{i-} = 0$	$\phi^{i+} - \phi^{i-} = 0$	$\phi^{i+} = 0; \phi^{i-} = 0$	
3	$u_1^{i+} - u_1^{i-} = 0$	$u_2^{i+} - u_2^{i-} = 0$	$u_3^{i+} - u_3^{i-} = q$	-	$c_{3j}^E = \bar{T}_j/\bar{S}_3$ (10)
	-	$\phi^{i+} - \phi^{i-} = 0$	$\phi^{i+} - \phi^{i-} = 0$	$\phi^{i+} = 0; \phi^{i-} = 0$	
4	$u_1^{i+} - u_1^{i-} = 0$	$u_3^{i+} - u_3^{i-} = q$	$u_2^{i+} - u_2^{i-} = q$	-	$c_{44}^E = \bar{T}_4/\bar{S}_4$ (11)
	-	$\phi^{i+} - \phi^{i-} = 0$	$\phi^{i+} - \phi^{i-} = 0$	$\phi^{i+} = 0; \phi^{i-} = 0$	
5	$u_3^{i+} - u_3^{i-} = q$	$u_2^{i+} - u_2^{i-} = 0$	$u_1^{i+} - u_1^{i-} = q$	-	$c_{55}^E = \bar{T}_5/\bar{S}_5$ (11)
	-	$\phi^{i+} - \phi^{i-} = 0$	$\phi^{i+} - \phi^{i-} = 0$	$\phi^{i+} = 0; \phi^{i-} = 0$	$e_{15} = \bar{D}_1/\bar{S}_5$ (12)
6	$u_2^{i+} - u_2^{i-} = q$	$u_1^{i+} - u_1^{i-} = q$	$u_3^{i+} - u_3^{i-} = 0$	-	$c_{66}^E = \bar{T}_6/\bar{S}_6$ (11)
	-	$\phi^{i+} - \phi^{i-} = 0$	$\phi^{i+} - \phi^{i-} = 0$	$\phi^{i+} = 0; \phi^{i-} = 0$	
7	-	-	-	-	$d_{15} = \bar{S}_5/\bar{E}_1$ (13)
	-	$\phi^{i+} - \phi^{i-} = 0$	$\phi^{i+} - \phi^{i-} = 0$	$\phi^{i+} = 0; \phi^{i-} = q$	$\epsilon_{11}^T = \bar{D}_1/\bar{E}_1$ (13)

For both the previous cases, equations (10) and (11), to ensure a short circuit electric boundary condition, the voltage degrees of freedom in the electrodes at surfaces X_1^{e-} and X_1^{e+} are set to zero. Table 2 indicates symmetric boundary conditions for the electric potential along directions x_2 and x_3 for the corresponding X_2^-/X_2^+ and X_3^-/X_3^+ RVE surfaces.

The piezoelectric constant e_{15} can be also obtained from the local problem used to evaluate c_{55}^E, which is where a pure shear stress state in the plane $x_1 - x_3$ is approximated. From the constitutive equations (1), e_{15} can be obtained by evaluating the average electric displacement D_1 such that

$$e_{15} = \bar{D}_1/\bar{S}_5. \qquad (12)$$

where the average shear strain $\bar{S}_5$ and electric displacement $\bar{D}_1$ are evaluated using the approximation of (8) and (9).

For the evaluation of the piezoelectric and dielectric constants of the d-form, d_{15} and ϵ_{11}^T, another local problem is set up for which an electric voltage $\phi^{X_1^{e+}} = h_P$ (in value) is applied to the electrode at surface X_1^{e+} ($x_1 = h_P + h_E + h_A + h_K$) while the voltage at the opposite electrode (at surface X_1^{e-}, $x_1 = h_E + h_A + h_K$) is set to zero so that a unitary electric field in the x_1 direction is generated. To approximate the condition of zero stresses in the RVE, no restriction is made to the displacements in the RVE except for the origin where all displacements are set to zero to prevent rigid body displacements. Then, considering zero shear stress T_5 in the d-form of the constitutive equations, the piezoelectric and dielectric constants, d_{15} and ϵ_{11}^T, can be evaluated from

$$d_{15} = \bar{S}_5/\bar{E}_1 \text{ and } \epsilon_{11}^T = \bar{D}_1/\bar{E}_1. \qquad (13)$$

Table 2 summarizes the local problems used for the characterization of the relevant material properties of the d_{15} MFC RVE. u_j^{i-} and u_j^{i+} are the displacements in direction j and ϕ^{i-} and ϕ^{i+} are the electric potentials at i-th node of opposite surfaces. q is an arbitrary non-null value.

d_{15} MFC Effective Material Properties Evaluation

Figure 3 shows the finite element mesh used in Ansys$^{(R)}$ for the 7-layered d_{15} MFC RVE using a FVF of 0.86 for the PZT+Epoxy Active Layer. The 3D 20-Node coupled-field solid finite element SOLID226 was used to mesh all volumes. It has the three displacement translations along the Cartesian coordinate system and the electric

potential as nodal degrees of freedom. 5525 finite elements were used considering 25 divisions in x_1 direction (13 divisions for the PZT layer and 2 divisions for each electrode and protective layer), 13 divisions in x_2 direction and 17 divisions in x_3 direction (11 divisions for the PZT layer and 3 divisions for each Epoxy layer). According to Fig. 2, the dimensions considered for this RVE are $h_P = 1$ mm, $h_K = 25.4$ μm, $h_A = 12.7$ μm and $h_E = 17.8$ μm, $L_P = 0.860$ mm, $L_E = 0.140$ mm and $w = 1$ mm (Raja and Ikeda, 2008). The material properties for the piezoceramic material Sonox P502, taken from Deraemaeker et al. (2009), are: $s_{11}^E = s_{22}^E = 18.5$ pm²/N, $s_{33}^E = 20.7$ pm²/N, $s_{12}^E = -6.29$ pm²/N, $s_{13}^E = -6.23$ pm²/N, $s_{44}^E = s_{55}^E = 33.2$ pm²/N, $s_{66}^E = 52.3$ pm²/N, $d_{31} = d_{32} = -185$ pC/N, $d_{33} = 440$ pC/N, $d_{15} = d_{24} = 560$ pC/N, $\epsilon_{11}^T = \epsilon_{22}^T = 1950\epsilon_0$, $\epsilon_{33}^T = 1850\epsilon_0$. The material properties for the isotropic Epoxy are: $Y = 2.9$ GPa, $\nu = 0.3$ and $\epsilon = 4.25\epsilon_0$. The materials properties for the protective layers, taken from Raja and Ikeda (2008), are: Kapton – $Y = 2.5$ GPa, $\nu = 0.34$ and $\epsilon = 3.4\epsilon_0$ and Acrylic – $Y = 2.7$ GPa, $\nu = 0.35$ and $\epsilon = 3.4\epsilon_0$. The material properties for the Copper electrode are: $Y = 117$ GPa, $\nu = 0.35$ and $\epsilon = 5\epsilon_0$.
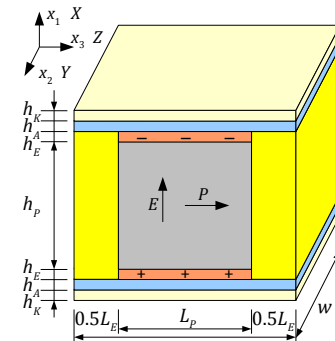

Figure 2. Representative volume element (RVE) for a d_{15} MFC.

Table 3 shows the effective properties, transformed to Voigt notation, of the d_{15} MFC, active layer only (columns 1 and 3) and full 7-layer composite (columns 2 and 4), using FVF of 0.86 and 0.95 obtained by the finite element local problems. The effective electromechanical coupling coefficient of the RVE k_{15} is evaluated from the effective elastic, piezoelectric and dielectric properties, c_{55}^E, d_{15} and ϵ_{11}^T, using (2). The results for the active layer only were validated in a previous work (Trindade and Benjeddou, 2011) through comparison with those obtained by analytical homogenization methods UFM (without the unidirectional electric field, UDEF, approximation) and AHM (with the UDEF

Table 3. Effective short-circuit material properties of d_{15} MFC and its active layer for two fibre volume fractions.

| FVF = 0.86		FVF = 0.95	
MFC active layer	7-layers MFC	MFC active layer	7-layers MFC
$Y_1 = 50.09$ GPa	$Y_1 = 26.43$ GPa	$Y_1 = 54.81$ GPa	$Y_1 = 28.72$ GPa
$Y_2 = 50.09$ GPa	$Y_2 = 48.44$ GPa	$Y_2 = 54.81$ GPa	$Y_2 = 53.00$ GPa
$Y_3 = 20.53$ GPa	$Y_3 = 19.84$ GPa	$Y_3 = 37.41$ GPa	$Y_3 = 35.71$ GPa
$G_{23} = 6.49$ GPa	$G_{23} = 6.33$ GPa	$G_{23} = 13.09$ GPa	$G_{23} = 12.58$ GPa
$G_{13} = 6.49$ GPa	$G_{13} = 4.73$ GPa	$G_{13} = 13.09$ GPa	$G_{13} = 7.09$ GPa
$G_{12} = 16.60$ GPa	$G_{12} = 7.64$ GPa	$G_{12} = 18.22$ GPa	$G_{12} = 8.16$ GPa
$\nu_{12} = 0.43$	$\nu_{12} = 0.23$	$\nu_{12} = 0.43$	$\nu_{12} = 0.23$
$\nu_{13} = 0.20$	$\nu_{13} = 0.15$	$\nu_{13} = 0.21$	$\nu_{13} = 0.13$
$\nu_{23} = 0.20$	$\nu_{23} = 0.22$	$\nu_{23} = 0.21$	$\nu_{23} = 0.22$
$d_{15} = 486.67$ pC/N	$d_{15} = 485.60$ pC/N	$d_{15} = 532.61$ pC/N	$d_{15} = 532.60$ pC/N
$e_{15} = 3.13$ C/m^2	$e_{15} = 2.06$ C/m^2	$e_{15} = 6.97$ C/m^2	$e_{15} = 3.40$ C/m^2
$\epsilon_{11}^T = 15.01$ nF/m	$\epsilon_{11}^T = 14.95$ nF/m	$\epsilon_{11}^T = 16.42$ nF/m	$\epsilon_{11}^T = 16.41$ nF/m
$k_{15}^2 = 10.2$ %	$k_{15}^2 = 7.5$ %	$k_{15}^2 = 22.6$ %	$k_{15}^2 = 12.2$ %
$k_{15} = 0.32$	$k_{15} = 0.27$	$k_{15} = 0.48$	$k_{15} = 0.35$
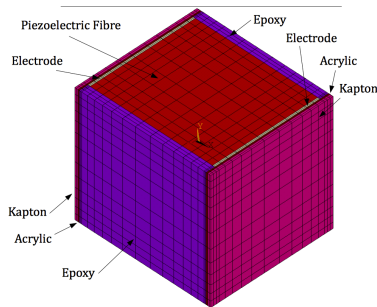
Figure 3. Finite element mesh for the 7-layered d_{15} MFC RVE with FVF = 0.86.

approximation) (Benjeddou and Al-Ajmi, 2009). Notice however that, in Trindade and Benjeddou (2011), an equivalent homogeneous electrode layer (80% Copper, 20% Epoxy) was considered, whose properties were evaluated using mixture laws, whereas, in the present case, the electrode layer is heterogeneous (Epoxy/Copper/Epoxy) and the Copper portion covers only the piezoceramic fibre, as shown in Figs. 1(b) and 2. The present results are almost exactly the same as in Trindade and Benjeddou (2011).

The results show that the increase in the FVF from 0.86 to 0.95, meaning a 10% increase, leads to an overall increase in the elastic (stiffness) constants. More importantly, the effective piezoelectric properties of major interest to the d_{15} MFC, d_{15} or e_{15}, increase substantially by 10% and 123%, respectively, for the active layer. This yields an increase in the effective squared electromechanical coupling coefficient k_{15}^2 by 123%, from 10% to 23%, for the active layer.

Table 3 also shows that, while the active layer is almost transversally isotropic, the 7-layered composite is definitely orthotropic. In particular, the Young modulus Y_1 is significantly diminished due to the relatively soft protective layers. On the other hand, the Young modulus Y_3 is little decreased mainly due to the electrode that is stiffer than the PZT core and thus promotes a stiffer connection between the X_3^+ surface and the PZT core. The shear modulus G_{13} is diminished by 27% (for FVF 0.86) and 46% (for FVF 0.95) due to the protective layers which are softer than the PZT. Notice, however, that the thickness of the protective and electrode layers should also play a major role in this shear modulus, for instance a decrease on the thickness of these layers should increase the shear modulus G_{13}, but will also perform poorly as protective layers. The piezoelectric constant d_{15} is decreased a little while e_{15}

is decreased by 30%, from 3.13 to 2.06 C/m^2. The dielectric constant ϵ_{11}^T is not modified due to the protective and electrode layers, since it is assumed that the electric contact between electrode and PZT occurs at the PZT-electrode interface. This would not be the case if there should be an epoxy layer between Copper electrode and PZT. These effective properties yield an overall smaller electromechanical coupling coefficient k_{15}, such that the efficiency in energy conversion k_{15}^2 decreases by 20%, from 10% to 8%. Notice that this is much less than the k_{15}^2 of the PZT (Sonox P502) alone of 54.8%.

Parametric Analysis

In the previous section, it was noticed that, besides the fibre volume fraction, the packaging design may affect significantly the performance of the MFC transducer. In particular, the softer materials that provide the desired flexibility for the transducer also decrease its performance. Therefore, it is of great interest to analyse the effect of the variation of material and geometrical properties of the MFC on its effective material properties.

In particular, it was observed that the Epoxy material is the main responsible for the decrease of MFC stiffness and, thus, actuation authority represented by the piezoelectric stress constant e_{15}. The MFC effective stiffness may be controlled through either the fibre volume fraction or the Epoxy material stiffness constants, such that an increase of any of them should lead to an increase on the MFC effective stiffness. Thus, in this section, the effect of variations of both fibre volume fraction and Epoxy Young's modulus is analysed.

On the other hand, the electrode and protective layers also strongly affect the MFC effective material properties, as it can be noticed from the comparison between active layer only and 7-layers MFC of previous section (Table 3). In particular, the materials used for the protective layers are very soft (Epoxy-like stiffness) while the Copper used for the electrode layer is quite stiff. Thus, the effect of variations of electrode layer thickness is also analyzed.

Finally, the active layer thickness is also an interesting parameter since it can be designed for a particular application without significant modification of the packaging design. Therefore, it is also worthwhile to analyze its effect on the transducer performance.

Hence, this section presents a parametric analysis of the d_{15} MFC effective material properties by varying the following selected parameters (one at a time): i) active layer fibre volume fraction, ii) Epoxy elastic modulus, iii) Copper electrode thickness, and iv) active layer thickness. Unless stated otherwise, the default values for the parameters are those presented in the previous section. The fibre
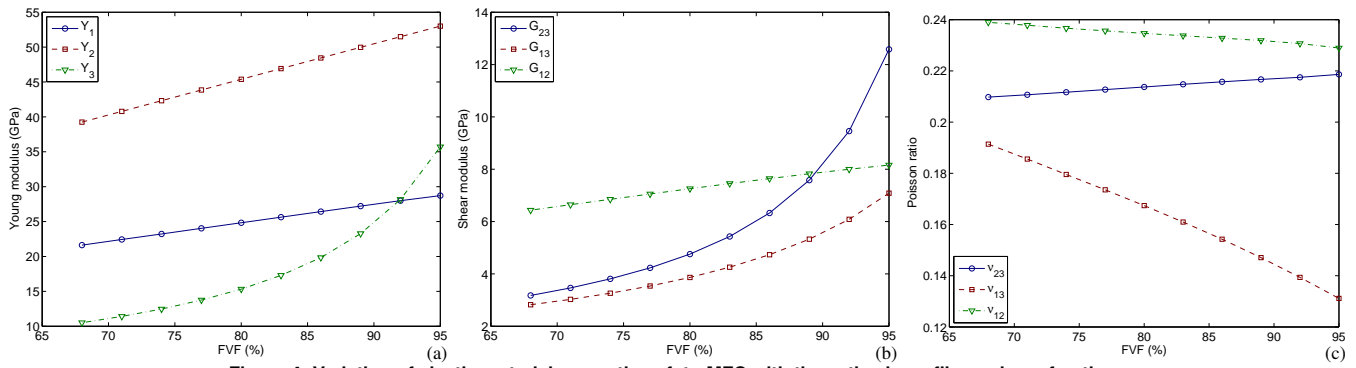
Figure 4. Variation of elastic material properties of d_{15} MFC with the active layer fibre volume fraction.
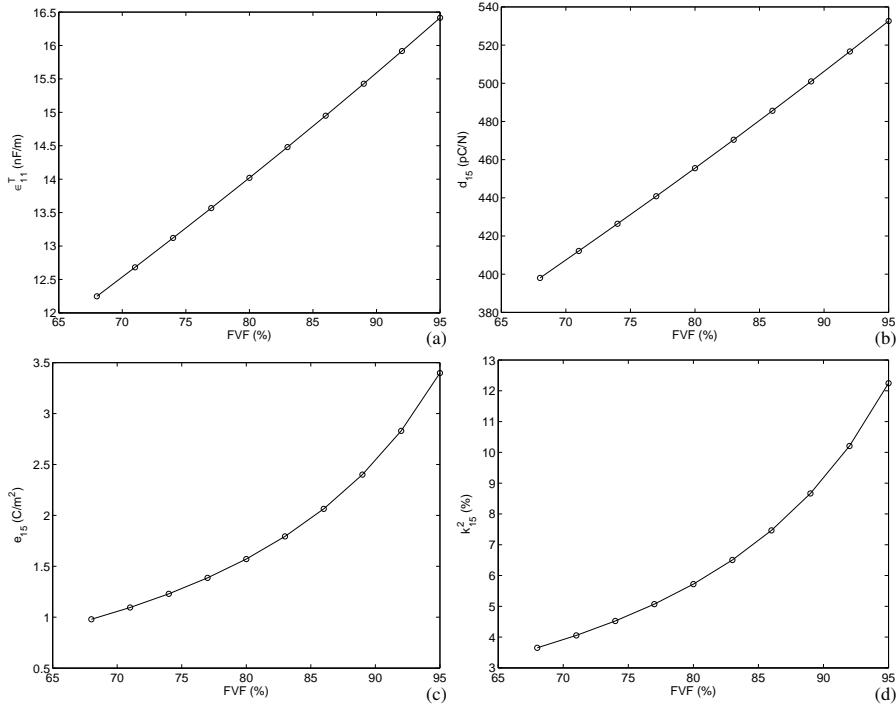

Figure 5. Variation of dielectric, piezoelectric and electromechanical coupling material properties of d_{15} MFC with the active layer fibre volume fraction.

volume fraction varies from 68% to 95% with 3% increments. The Epoxy elastic modulus is decreased/increased by 10% and 20% from the standard value used in the previous section ($Y_E = 2.9$ GPa). The Copper electrode thickness is also decreased/increased by 10% and 20% from the value of the previous section ($h_E = 17.8$ μm). As for the active layer thickness, it varies from 0.25 mm to 1.0 mm with 0.25 mm increments. Notice that, for each parameter set, the seven local problems presented previously (Table 2) are solved and the corresponding effective material properties are evaluated.

In a first analysis, the fibre volume fraction varies in the range from 68% to 95%. Notice that the standard piezoelectric MFC are manufactured using a 86% FVF (Deraemaecker et al., 2007). As expected, all elastic stiffness coefficients increase for higher FVF, since the piezoceramic is much stiffer than the Epoxy (Fig. 4). A more detailed analysis shows, however, that whereas constants Y_1, Y_2 and G_{12} increase linearly with the FVF, the other elastic stiffness constants Y_3, G_{23} and G_{13} present a non-linear augmentation, as shown in Fig. 4. On the other hand, the Poisson ratios ν_{13} and ν_{12} decrease with increasing FVF and ν_{23} increases moderately. As shown in Fig. 5, the piezoelectric and dielectric material properties

increase substantially for higher FVF, since those are only due to the piezoelectric part of the active layer. It can be observed from Fig. 5 that ϵ_{11}^T and d_{15} (dielectric and piezoelectric) constants increase linearly with FVF, while piezoelectric constant e_{15} and squared electromechanical coupling coefficient k_{15}^2 increase rates augment with FVF, indicating that maximization of FVF is more important for applications using the d_{15} MFC as actuators or energy converters.

In a second analysis, the effect of the Epoxy elastic modulus on the effective material properties is analyzed. Since the major part of elastic strains is concentrated in the Epoxy material, it is expected that stiffer Epoxy materials could improve both overall stiffness and electromechanical coupling. Indeed, as shown in Fig. 6(a), an increase of 20% on the Epoxy elastic modulus, relative to the standard value $Y_E = 2.9$ GPa, leads to an increase of almost 15% on d_{15} MFC elastic constant Y_3. On the other hand, effective elastic constants Y_1 and Y_2 are not significantly altered by the Epoxy elastic modulus. As for the shear elastic constants, G_{23} and G_{13} increase by around 15% and 10%, respectively, when Epoxy elastic modulus is increased by 20% while constant G_{12} remains nearly unchanged (Fig. 6(b)). The Poisson ratios vary by less than 5% as shown in Fig. 6(c).
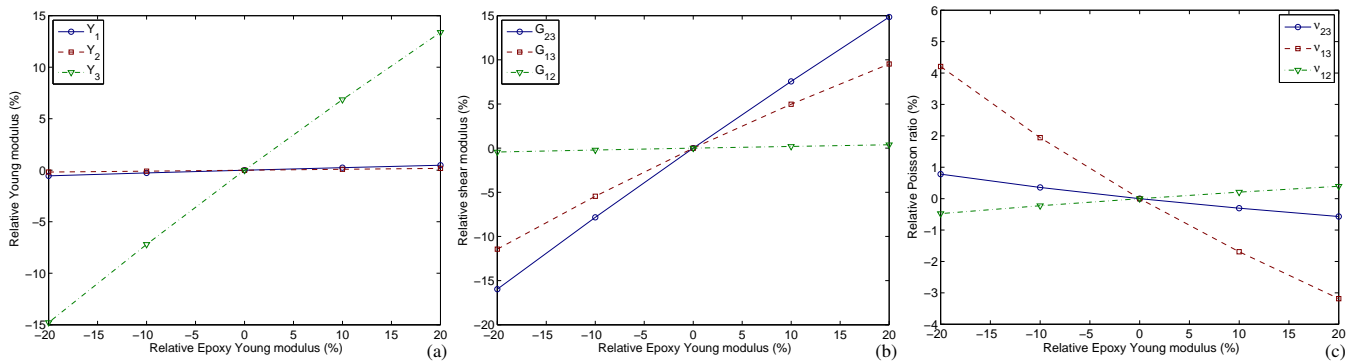
Figure 6. Variation of elastic material properties of d_{15} MFC with Epoxy elastic modulus.
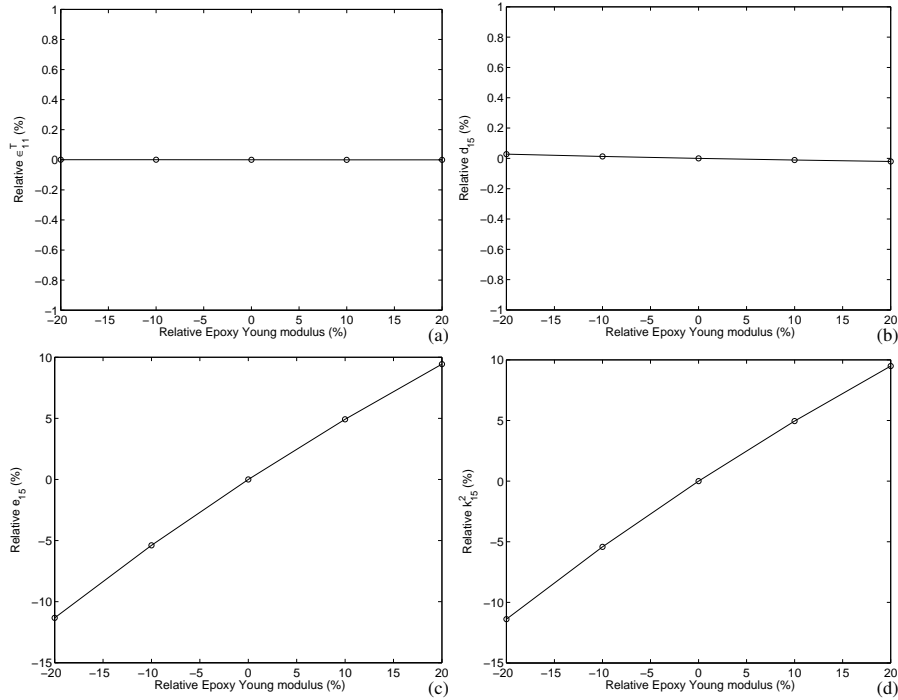

Figure 7. Variation of dielectric, piezoelectric and electromechanical coupling material properties of d_{15} MFC with Epoxy elastic modulus.

On the other hand, the dielectric constant ϵ_{11}^T of the d_{15} MFC is not affected by the variation of Epoxy elastic modulus (Fig. 7(a)). The same happens to piezoelectric constant d_{15} (Fig. 7(b)). However, the piezoelectric constant e_{15}, which depends on the effective shear stiffness of the composite, increases approximately by 10% when the Epoxy elastic modulus is increased by 20%, as shown in Fig. 7(c). A very similar dependence is observed for the squared electromechanical coupling coefficient k_{15}^2, shown in Fig. 7(d). This indicates that stiffer Epoxy materials should be more interesting for actuators and energy converters applications. Notice, however, that this would also lead to a less flexible (conformable) transducer.

From previous analyses, it seemed that electrode thickness could affect the effective material properties of the d_{15} MFC, since this layer responds to the major part of the covering layer (electrode and Kapton/Acrylic protective layers) stiffness. Therefore, this property was also varied in the range ±20%. Since a Copper electrode is commonly used, it did not seem appropriate to vary its elastic modulus. For the same reason, the Kapton and Acrylic protective layers material properties were also kept unchanged. Figure 8 shows that an increase of the electrode thickness yields an overall augmentation of the d_{15} MFC stiffness constants, although this augmentation is smaller than 1%. Elastic constants Y_1, Y_2 and G_{12} are the most affected by the electrode thickness variation. Poisson ratios are not significantly affected. As for the variation of the previous parameter, dielectric constant ϵ_{11}^T and piezoelectric constant d_{15} are not affected by the variation of electrode thickness. On the other hand, the piezoelectric constant e_{15} decreases a little (0.4%), while the squared electromechanical coupling coefficient k_{15}^2 increases a little (0.2%), for an increase of 20% in the electrode thickness (Fig. 9).

In the last parametric analysis, the active layer thickness varies in the range [0.25-1.00] mm while maintaining the other parameters unchanged. Notice that this parameter could also affect the coupling with the external (host) structure since it modifies the transducer geometry and, thus, its effective performance. Nevertheless, the reduction of active layer thickness also leads to a decrease of the active part in relation to the MFC packaging and, thus, it is worthwhile analysing the effect of this variation on the MFC effective properties.

As shown in Fig. 10, both Young and shear moduli augment for increasing active layer thickness. Constants Y_1, G_{12} and ν_{12} are the most affected by this variation. The dielectric constant ϵ_{11}^T
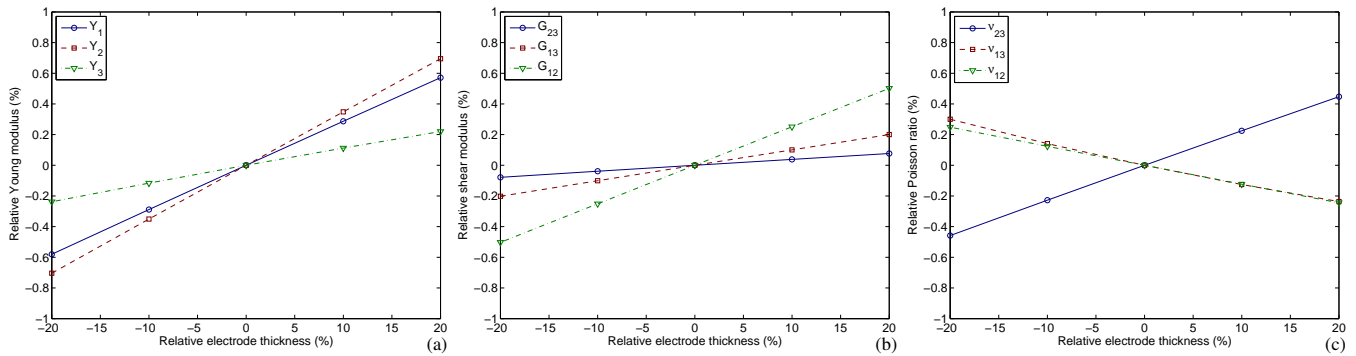
Figure 8. Variation of elastic material properties of d_{15} MFC with electrode thickness.
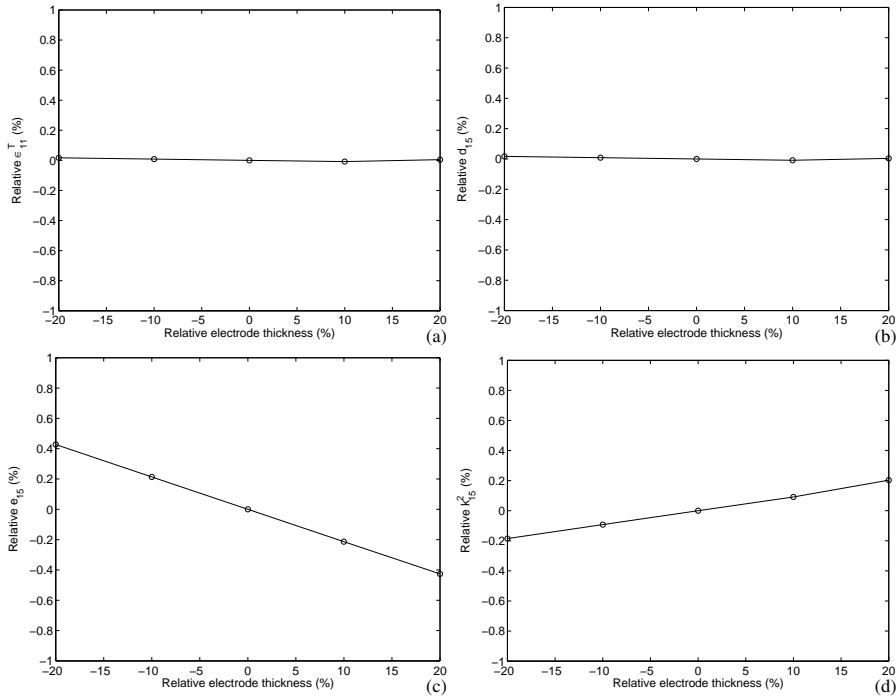

Figure 9. Variation of dielectric, piezoelectric and electromechanical coupling material properties of d_{15} MFC with electrode thickness.
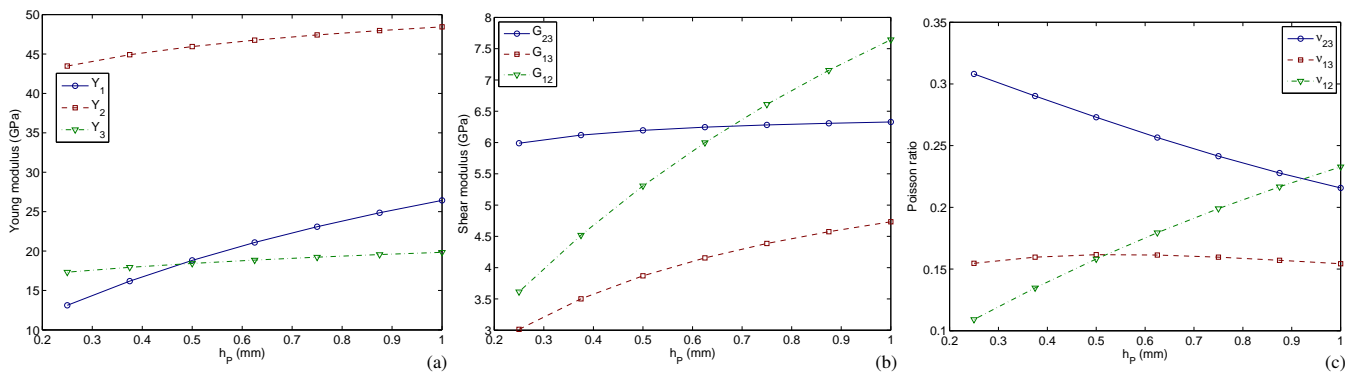

Figure 10. Variation of elastic material properties of d_{15} MFC with active layer thickness.

and piezoelectric charge constant d_{15} are not much affected by the variation of the active layer thickness, increasing around 2% for a decrease on the active layer thickness from 1 mm down to 0.25 mm (Figs. 11(a) and 11(b)). On the other hand, both piezoelectric stress constant e_{15} and squared electromechanical coupling coefficient k_{15}^2 increase substantially for increasing active layer thickness, around

100% for e_{15} and 50% for k_{15}^2 (Figs. 11(c) and 11(d)).

Concluding Remarks

This work presented a parametric analysis of the effective material properties of a d_{15} thickness-shear piezoelectric Macro-
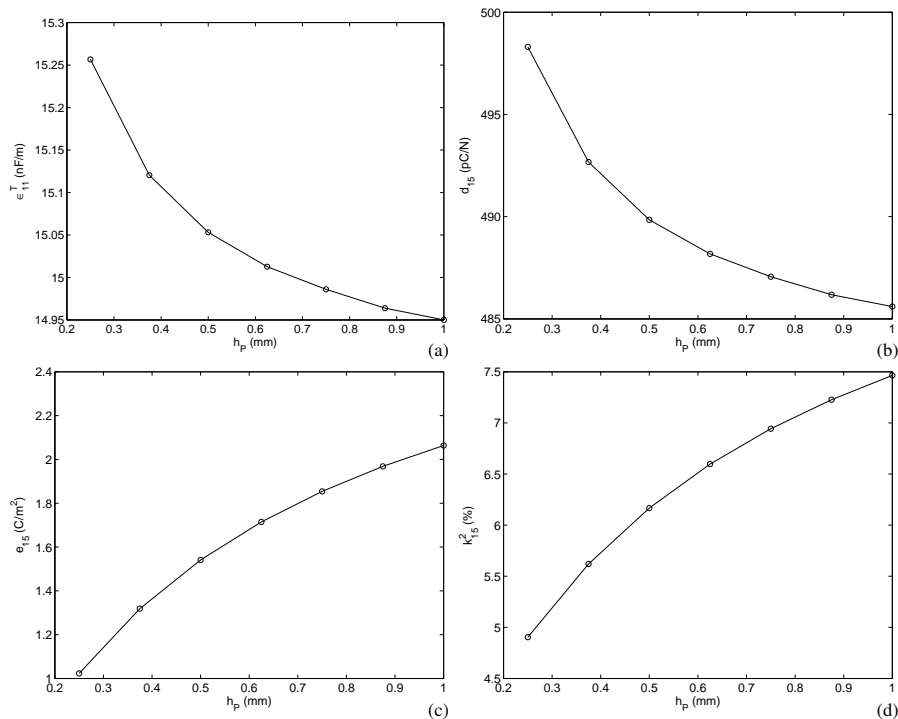
Figure 11. Variation of dielectric, piezoelectric and electromechanical coupling material properties of d_{15} MFC with active layer thickness.

Fibre Composite (MFC) made of seven layers (Kapton, Acrylic, Electrode, Piezoceramic Fibre and Epoxy Composite, Electrode, Acrylic, Kapton). It confirms that the MFC packaging reduces significantly the shear stiffness of the piezoceramic material and, thus, leading to significantly smaller effective electromechanical coupling coefficient k_{15} and piezoelectric stress constant e_{15} when compared to the piezoceramic fibre properties. The effect of the variations of fibre volume fraction, Epoxy elastic modulus, electrode thickness and active layer thickness on the MFC effective material properties was evaluated. Results indicated that an effective d_{15} MFC should use relatively thick fibres having relatively high shear modulus and relatively stiff epoxy filler. On the other hand, it was found that the electrode thickness does not affect significantly the MFC performance.

Acknowledgements

References

Baillargeon, B.P. and Vel, S.S., 2005, "Exact solution for the vibration and active damping of composite plates with piezoelectric shear actuators," *Journal of Sound and Vibration*, Vol. 282, pp. 781-804.

Benjeddou, A. and Al-Ajmi, M., 2009, "Analytical homogenizations of piezoceramic d_{15} shear macro-fibre composites," Proceedings of the IUTAM Conference on Multiscale Modelling of Fatigue, Damage and Fracture in Smart Materials, eds. M. Kuna and A. Ricoeur (Freiberg, Germany), Sept 1-4.

Benjeddou, A. and Ranger, J-A., 2006, "Use of shunted shear-mode piezoceramics for structural vibration passive damping," *Computers and Structures*, Vol. 84, pp. 1415-1425.

Benjeddou, A., 2007, "Shear-mode piezoceramic advanced materials and structures: A state of the art," *Mechanics of Advanced Materials and Structures*, Vol. 14, No. 4, pp. 263-275.

Benjeddou, A., Trindade, M.A. and Ohayon, R., 1997, "A unified beam finite element model for extension and shear piezoelectric actuation mechanisms," *Journal of Intelligent Material Systems and Structures*, Vol. 8, No. 12, pp. 1012-1025.

Benjeddou, A., Trindade, M.A. and Ohayon, R., 2000, "Piezoelectric actuation mechanisms for intelligent sandwich structures," *Smart Materials and Structures*, Vol. 9, No. 3, pp. 328-335.

Bent, A.A. and Hagood, N.W., 1997, "Piezoelectric fiber composites with interdigitated electrodes," *Journal of Intelligent Material Systems and Structures*, Vol. 8, pp. 903-919.

Berger, H., Kari, S., Gabbert, U., Rodriguez-Ramos, R., Guinovart, R., Otero, J.A. and Bravo-Castirello, J., 2005, "An analytical and numerical approach for calculating effective material coefficients of piezoelectric fiber composites," *International Journal of Solids and Structures*, Vol. 42, pp. 5692-5714.

Biscani, F., Nasser, H., Belouettar, S. and Carrera, E., 2011, "Equivalent electro-elastic properties of Macro Fiber Composite (MFC) transducers using asymptotic expansion approach," *Composites: Part B*, Vol. 42, No. 3, pp. 444-455.

Deraemaeker, A. and Nasser, H., 2010, "Numerical evaluation of the equivalent properties of Macro Fiber Composite (MFC) transducers using periodic homogenization," *International Journal of Solids and Structures*, Vol. 47, No. 24, pp. 3272-3285.

Deraemaeker, A., Benelechi, S., Benjeddou, A. and Preumont, A., 2007, "Analytical and numerical computation of homogenized properties of MFCs: Application to a composite boom with MFC actuators and sensors," III ECCOMAS Thematic Conference on Smart Structures and Materials, eds. W. Ostachowicz et al. (Gdansk, Poland), July 9-11.

Deraemaeker, A., Nasser, H., Benjeddou, A. and Preumont, A., 2009, "Mixing rules for the piezoelectric properties of macro fiber composites," *Journal of Intelligent Material Systems and Structures*, Vol. 20, No. 12, pp. 1475-1482.

Ikeda, T., 1990, "Fundamentals of Piezoelectricity," Oxford University Press.

Otero, J.A., Rodriguez-Ramos, R., Monsivais, G. and Perez-Alvarez, R., 2005, "Dynamical behavior of a layered piezocomposite using the asymptotic homogenization method," *Mechanics of Materials*, Vol. 37, pp. 33-44.

Raja, S. and Ikeda, T., 2008, "Concept and electro-elastic modeling of shear actuated fiber composite using micro-mechanics approach," *Journal of Intelligent Material Systems and Structures*, Vol. 19, pp. 1173-1183.

Raja, S., Ikeda, T. and Dwarakanathan, D., 2011, "Deflection and

vibration control of laminated plates using extension and shear actuated fiber composites," *Smart Materials Research*, Vol. 2011, Art. No. 515942.

Raja, S., Prathap, G. and Sinha, P.K., 2002, "Active vibration control of composite sandwich beams with piezoelectric extension-bending and shear actuators," *Smart Materials and Structures*, Vol. 11, No. 1, pp. 63-71.

Santos, H.F.L. and Trindade, M.A., 2011, "Structural vibration control using extension and shear active-passive piezoelectric networks including sensitivity to electrical uncertainties," *Journal of the Brazilian Society of Mechanical Sciences and Engineering*, Vol. 33, No. 3, pp. 287-301.

Skinner, D.P., Newnham, R.E. and Cross, L.E., 1978, "Flexible composite transducers," *Materials Research Bulletin*, Vol. 13, pp. 599-607.

Sun, C.T. and Zhang, X.D., 1995, "Use of thickness-shear mode in adaptive sandwich structures," *Smart Materials and Structures*, Vol. 4, No. 3, pp. 202-206.

Trindade, M.A. and Benjeddou, A., 2009, "Effective electromechanical coupling coefficients of piezoelectric adaptive structures: critical evaluation and optimization," *Mechanics of Advanced Materials and Structures*, Vol. 16, No. 3, pp. 210-223.

Trindade, M.A. and Benjeddou, A., 2011, "Finite element homogenization technique for the characterization of d15 shear piezoelectric macro-fibre composites," *Smart Materials and Structures*, Vol. 20, No. 7, Art. No. 075012.

Trindade, M.A. and Maio, C.E.B., 2008, "Multimodal passive vibration control of sandwich beams with shunted shear piezoelectric materials," *Smart Materials and Structures*, Vol. 17, Art. No.055015.

Trindade, M.A., 2011, "Experimental analysis of active-passive vibration control using viscoelastic materials and extension and shear piezoelectric actuators," *Journal of Vibration and Control*, Vol. 17, No. 6, pp. 917-929.

Wilkie, W.K., Bryant, G.R. and High, J.W., 2000, "Low-cost piezocomposite actuator for structural control applications," Proceedings of SPIE International Symposium on Smart Structures and Materials, Newport Beach, 5-9 March.